Deletion of the *miR-144/451* cluster aggravates lethal sepsis-induced lung epithelial oxidative stress and apoptosis

Fan Wu[1,2#], Xiaoling Yuan[3#], Weili Liu[1,4#], Lijun Meng[1,4], Xiuru Li[1], Xiang Gao[1], Shuting Zhou[1,2], Lei Fang[1,2], Duonan Yu[1,2,4]

[1]Institute of Translational Medicine, Medical College, Yangzhou University, Yangzhou, China; [2]Jiangsu Key Laboratory of Experimental & Translational Non-coding RNA Research, Yangzhou, China; [3]Children Rehabilitation Department, Yangzhou Maternal and Child Health Hospital, Yangzhou, China; [4]Intensive Care Unit, Affiliated Hospital of Yangzhou University, Yangzhou, China

Contributions: (I) Conception and design: L Fang, D Yu; (II) Administrative support: D Yu; (III) Provision of study materials: W Liu, L Fang, D Yu; (IV) Collection and assembly of data: F Wu, X Yuan, L Meng, X Li, X Gao; (V) Data analysis and interpretation: F Wu, X Li, X Gao, S Zhou; (VI) Manuscript writing: All authors; (VII) Final approval of manuscript: All authors.

[#]These authors contributed equally to this work.

Correspondence to: Professor Duonan Yu. Jiangsu Key Laboratory of Experimental & Translational Non-coding RNA Research, Yangzhou University Medical College, Yangzhou 225009, China. Email: dnyu@yzu.edu.cn; Lei Fang, PhD. Institute of Translational Medicine, Medical College, Yangzhou University, Yangzhou 225009, China. Email: fanglei@yzu.edu.cn.

Background: Sepsis is associated with a high mortality rate. A major cause of death in sepsis patients is respiratory failure, which is characterized by oxidative injury, epithelial apoptosis, and increased lung permeability. MicroRNAs (miRs) are important regulators of sepsis progression.

Methods: This study aimed to explore the role of *miR-144/451* in sepsis in mice. Experimental sepsis was induced in C57BL/6 mice by cecal ligation and puncture (CLP).

Results: CLP significantly induced systemic inflammation, lung permeability, and lung epithelial apoptosis with downregulated messenger RNA (mRNA) levels of antioxidant enzymes. The *miR-144/451* knockout mice had a lower 48-hour survival rate, higher plasma tumor necrosis factor α (TNF-α) and interleukin-6 (IL-6) levels, and greater pulmonary permeability compared with wild-type mice after CLP. CLP also markedly increased interstitial hemorrhage, collapsed more alveolar sacs, and increased the number of terminal deoxynucleotidyl transferase dUTP nick-end labeling (TUNEL)-positive and Bcl-2-associated X (Bax)-positive cells in *miR-144/451* knockout lung tissues, with elevated mRNA levels of *Bax* and reduced activities of catalase (Cat), glutathione peroxidase 1(Gpx1). *MiR-451* negatively regulated 14-3-3ζ expression evidenced in *miR-144/451* knockout lungs and the A549 cell line. In lipopolysaccharide (LPS)-induced A549 cells, *miR-451* overexpression remarkably suppressed the production of reactive oxygen species, inhibited cell apoptosis, and enhanced levels of *FoxO3* protein and related enzymes.

Conclusions: Deletion of the *miR-144/451* cluster aggravated sepsis-induced oxidative injury of lung epithelial cells.

Keywords: *miR-144/451*; sepsis; epithelial; oxidative stress; apoptosis

Introduction

Sepsis is a general response to infection, affecting 20% of patients in intensive care units. Its 90-day mortality rate reaches 35.5% (1). Sepsis is characterized by a systemic inflammatory response (2). Uncontrolled inflammation often deleteriously affects the homeostasis of vital organs and ultimately evolves into multi-organ failure involving the pulmonary, circulatory, renal, gastrointestinal, hepatic, hematologic, and central nervous systems (3). Sepsis treatment includes supportive interventions such as antibiotics, mechanical ventilation, fluids, and vasopressors, but the mortality rate among hospitalized patients remain high (4).

The lungs are often the first organ to fail in response to sepsis (5), and development of acute respiratory distress syndrome is common in sepsis patients (6). Clinical manifestations include pulmonary edema, reduced lung compliance, and severe hypoxemia (7). Lung epithelial cells, including airway and alveolar epithelial cells, are important for maintaining normal lung functions (8). The properties of lung epithelial cells can significantly impact the outcome of sepsis. Sepsis causes dysfunctions in the lung epithelium such as aberrant permeability, oxidative injury (9), and epithelial apoptosis (10). Oxidative stress occurs when the levels of oxidants exceed those of antioxidants and stimulates a cascade of lipid peroxidation reactions that initiate apoptosis and autophagy (11). Lung epithelial apoptosis impairs alveolar fluid clearance, prevents normal gas exchange, and exacerbates tissue hypoxia (12). In the later immunosuppression phase of sepsis, the lung tissue is susceptible to secondary infection (13), which aggravates oxidative stress and apoptosis. Prauchner *et al.* demonstrated that antioxidant supplementation (e.g., vitamin C and melatonin) is beneficial for sepsis treatment (14).

MicroRNAs (miRNAs) are a class of small, single-stranded noncoding RNAs that mediate posttranscriptional gene silencing, thereby regulating multiple biological activities (15). A number of studies have highlighted the critical functions played by miRNAs in modulating human respiratory diseases (16,17). *MiR-144/451* is a bicistronic miRNA gene locus that encodes two mature miRNAs: *miR-144* and *miR-451* (18). *MiR-144* is upregulated in lung epithelial cells of patients with chronic obstructive pulmonary disease, asthma, and pulmonary infection induced by the influenza virus (19-21), while *miR-451* in immune cells (dendritic cells or alveolar macrophages) prevents inflammatory lung injury (22,23). These studies strongly suggest that *miR-144/451* may be associated with the maintenance of lung homeostasis. Our previous studies revealed that *miR-451* protected erythrocytes against oxidant stress (18), and *miR-144/451* knockout (mKO) erythroblasts exhibited increased apoptosis during recovery from acute anemia (24). All published experiments on miR-144/451 function in lung injury were performed in cell lines or clinical samples. However, current study took advantage of our miR-144/451 knockout mouse model. The results from *in vivo* experiments are more convincing to support our conclusions. Here, we used mKO mice to ascertain whether *miR-144/451* improves lung epithelial oxidative stress and apoptosis in lethal sepsis. We present the following article in accordance with the ARRIVE reporting checklist (available at https://atm.amegroups.com/article/view/10.21037/atm-22-1024/rc).

Methods

Mice and cell lines

The mKO and wild-type (WT) mice used in this study have been described in our previous publications (24,25). Male mice (C57BL/6, 10–12 weeks old, 23–25 g) were used in this study. Experiments were performed under a project license (approval number: YXYLL-2019-64) granted by ethics committee of Yangzhou University, in compliance with National Institutes of Health Guidelines for the care and use of animals. A protocol was prepared before the study without registration. All the mice were kept in pathogen-free housing under a 12-hour light/dark cycle with free access to food and sterile water during the research procedures. The animals' health status was monitored throughout the experiments. A549 human pulmonary epithelial cell line and HEK293T packaging cell line were purchased from the Cell Bank of the Chinese Academy of Science (Shanghai, China).

Reagents

Mouse tumor necrosis factor α (TNF-α) and interleukin-6 (IL-6) enzyme-linked immunosorbent assay (ELISA kits) were obtained from Biolegend Co. (San Diego, CA, USA). An EL-TMB chromogenic reagent kit and primers for quantitative real-time polymerase chain reaction (qRT-PCR) were obtained from Sangon Biotech Co. (Shanghai, China). Evans blue dye and formamide were purchased from TCI Co. (Shanghai, China). Trizol, dichloro-

dihydro-fluorescein diacetate (DCFH-DA), bicinchoninic acid (BCA) protein assay kit, and Cell Counting Kit-8 (CCK-8) assay kit were obtained from Beyotime Biotechnology (Haimen, Jiangsu, China). Lipofectamine 2000 (Invitrogen Life Technologies, Carlsbad, CA, USA) was used for plasmid transfection. Transfection of the miRNA mimic was carried out using Lipo6000™ (Beyotime Biotechnology). Antibody against mouse 14-3-3ζ was purchased from Santa Cruz Biotechnology (Cat# SC-1019). FoxO3a (75D8) rabbit *monoclonal antibody* (mAb) was obtained from Cell Signaling Technology (Cat# 2497). Antibodies against tubulin (Cat#66031-1-Ig) and glyceraldehyde 3-phosphate dehydrogenase (GAPDH; Cat#60004-1-Ig) were obtained from Proteintech Group, Inc. (Rosemont, IL, USA). Enhanced chemiluminescence (ECL) reagent was purchased from Merck Millipore (Darmstadt, Germany). PrimeScript RT Master Mix was obtained from Takara Biotechnology (Dalian) Co., Ltd. (Dalian, Liaoning, China). HiScript III RT SuperMix for qPCR and ChamQ Universal SYBR qPCR Master Mix were purchased from Vazyme Biotech Co., Ltd. (Nanjing, Jiangsu, China). The streptavidin-biotin complex (SABC) immunohistochemistry (IHC) assay kit and 3,3'-Diaminobenzidine (DAB) color development kit were obtained from Boster Co. (Wuhan, Hubei, China). The terminal deoxynucleotidyl transferase-mediated dUTP nick end labeling (TUNEL) assay kit and nuclear and cytoplasmic protein extraction kit were purchased from KeyGen Biotech (Nanjing, Jiangsu, China). Annexin V-APC and propidium iodide (PI) were purchased from BD Biosciences (San Jose, CA, USA). Lipopolysaccharide (LPS) was purchased from Sigma-Aldrich (St. Louis, MO, USA). A *miR-451* mimic and its negative control (miR-NC) were purchased from GenePharma Co., Ltd. (Shanghai, China). The MSCV-PIG and MSCV-*miR-451* retroviral vectors have been described in our previous studies (24,25). All generic reagents were of analytical grade.

Murine model of polymicrobial sepsis induced by cecal ligation and puncture (CLP)

Mice were randomly assigned to 1 of 4 groups (n=6–8 each group): WT-sham, mKO-sham, WT-CLP, or mKO-CLP. Littermates were anaesthetized by intraperitoneal injection of pentobarbital sodium (50 mg/kg) and were subsequently subjected to high-grade CLP surgery as previously described (26). The abdominal muscles were incised and the cecum was exposed. The cecum was ligated at 6 mm from the tip using 3-0 silk sutures followed by a puncture with an 18-gauge needle to extrude a small amount of stool. Mice in the sham group underwent laparotomy without ligation or puncture. After CLP, the animals were monitored for 48 hours, and the survival rates were recorded.

Evaluation of lung permeability

Lung permeability was examined using the Evans blue dye extravasation method as previously described, with modifications (27). At 11.5 hours after CLP, mice were intravenously injected with Evans blue saline solution (30 mg/kg) via the tail vein. At 0.5 hours after Evans blue injection, mice were anesthetized by intraperitoneal injection of pentobarbital sodium and sacrificed by cervical dislocation. Immediately afterward, the lungs were perfused with 3 mL of phosphate-buffered saline (PBS) through the right ventricle, excised, and weighed. Lung samples were cut into pieces and Evans blue dye was extracted from the lung using 0.5 mL formamide for 24 hours at 60 ℃. Samples were then centrifuged at 2,000 ×g for 10 minutes at room temperature. Optical densities were measured using a microplate reader (Thermo Fisher Scientific, Waltham, MA, USA) at a wavelength of 630 nm. The amount of Evans blue dye in the lungs was calculated using a standard curve. Lung permeability was expressed as the amount of Evans blue dye per lung weight (μg/g).

TNF-α and IL-6 levels in plasma

At 12 hours after CLP, heparinized blood was collected from mice via retro-orbital vein puncture following intraperitoneal injection of pentobarbital sodium. The blood samples were centrifuged at 1,100 ×g for 10 minutes at 4 ℃. The levels of TNF-α and IL-6 in plasma samples were measured using ELISA.

Hematoxylin-eosin (HE), IHC staining, and TUNEL staining of lung tissues

The upper right lobes were fixed in 4% paraformaldehyde solution for 24 hours. Serial sections (4-μm-thick paraformaldehyde-fixed, paraffin-embedded) of lung tissues were stained with HE. To detect apoptosis, tissue sections were stained using the TUNEL staining reagent kit according to the manufacturer's instructions.

The sections were also subjected to IHC staining using the SABC IHC kit. The sections were deparaffinized,

rehydrated, and immersed in boiled citric acid buffer (pH 6.0) for thermal repair of antigens. After cooling down to room temperature, samples were incubated with 3% H_2O_2 for 10 minutes. After being washed with PBS, the sections were blocked with goat serum for 30 minutes and then incubated with a primary antibody against Bcl-2-associated X (Bax; 1:500) overnight at 4 ℃. The slides were incubated with biotinylated secondary antibody for 1 hour at room temperature, followed by incubation with streptavidin-horseradish peroxidase (HRP) for 30 minutes at room temperature. HRP signals were visualized using a DAB color development kit and counterstained with hematoxylin. The stained sections were observed under a microscope.

Lung catalase (CAT) and glutathione peroxidase 1 (Gpx1) activities

Lung samples from mice were homogenised in PBS (10% weight/volume solution), and Gpx1 activity was measured following the manufacturer's recommendations. Lung CAT activity was detected according to our previously reported method (28). Protein concentration in the tissue homogenate was measured using the BCA kit. CAT and Gpx1 activity in the lung tissues were expressed as U/mg protein.

Infection and LPS treatment of A549 cells

A549 and HEK293T cells were cultured in Dulbecco's Modified Eagle's Medium (DMEM) containing 1% glutamine and 10% *fetal bovine serum* (FBS) in a humidified 37 ℃ incubator with 5% CO_2. HEK293T cells were transfected with MSCV-PIG (Puromycin IRES GFP) and MSCV-*miR-451* plasmids using Lipofectamine 2000 as previously described (25). A549 cells were infected with retroviral supernatant from 293T packaging cells. Puromycin (1.6 μg/mL) was used for selection over a 3-day period. Puromycin-resistant cells were treated with LPS (8 μg/mL). Cell apoptosis, messenger RNA (mRNA) levels of apoptosis-related genes, and FoxO3 protein levels were then quantified.

Cell apoptosis

Cells were seeded at a density of 2.5×10^5 cells/mL in 6-well plates following LPS stimulation. After 24 hours, the cells were collected, centrifuged, and washed twice with cold PBS. The cells were then resuspended in binding buffer at a concentration of 10^6 cells/mL. For the cell apoptosis assay, 5 μL of Annexin V-APC and 5 μL of PI were added to the cells with incubation at room temperature for 15 minutes in the dark.

Reactive oxygen species (ROS) assays

The *miR-451* mimics and miR-NC were transfected into A549 cells using Lipo6000™ transfection reagent according to the manufacturer's instructions. Cells were incubated with DCFH-DA (10 μmol/L) at 37 ℃ for 30 minutes in the dark. DCF fluorescence intensities were analyzed using a FACSVerse and LSRFortessa Cell Analyzer System (BD Biosciences).

qRT-PCR

Total RNA was extracted from lung tissues or A549 cells using Trizol reagent. Complementary DNA (cDNA) was synthesized from 1 μg of total RNA using a reverse transcription kit according to the manufacturer's instructions. qRT-PCR was performed using the ABI 7500 Real-Time PCR system (Applied Biosystems, Foster City, CA, USA) with the following settings: 95 ℃ for 30 seconds, followed by 40 cycles of 95 ℃ for 10 seconds and 60 ℃ for 30 seconds. The relative RNA levels of *miR-451*, *Bcl2*, *Bax*, *Cat*, and *Gpx1* were calculated using the $2^{-\Delta\Delta Ct}$ formula with *U6* or *GAPDH* as internal references. The sequences of primers used in this study are listed in Table S1.

Western blot

Total protein was extracted from lung tissues or A549 cells using radioimmunoprecipitation assay (RIPA) lysis buffer containing a protease and phosphatase inhibitor cocktail. Protein concentration was determined using a BCA kit. Proteins were then separated by 10% sodium dodecyl sulfate polyacrylamide gel electrophoresis (SDS-PAGE) and transferred to a polyvinylidene difluoride (PVDF) membrane. The membrane was incubated with anti-14-3-3ζ and anti-FoxO3 antibodies overnight at 4 ℃. After being washed with PBS-Tween 3 times for 10 minutes, the membrane was incubated with HRP-conjugated secondary antibodies for 1 hour. The blots were visualized using the ECL method. AlphaView-Fluor Chem FC3 and ImageJ software were used for quantitative analysis of the protein intensity.
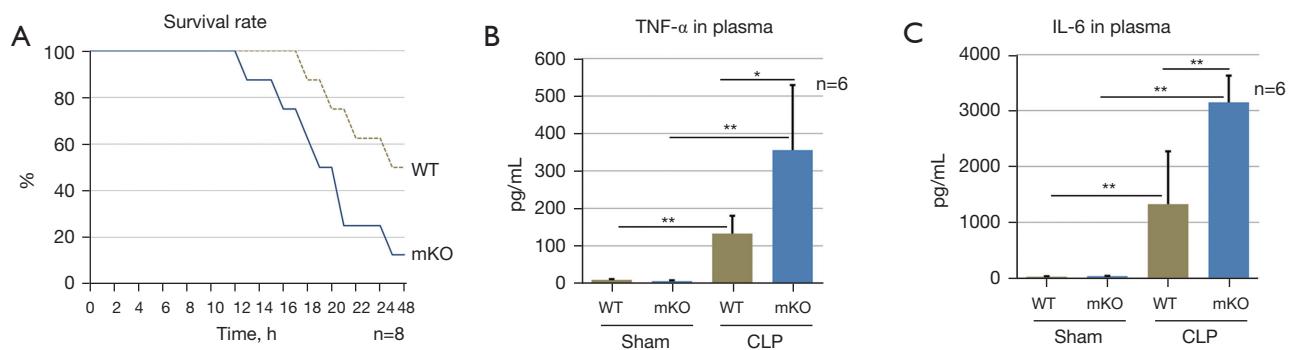
Figure 1 The sepsis survival rate and plasma levels of TNF-α and IL-6 in WT and mKO mice with CLP surgery. (A) The survival rate after 48 hours. Plasma TNF-α (B) and IL-6 (C) levels 12 hours post-CLP as determined by ELISA. Data are represented as means ± SD (n=8). *P<0.05; **P<0.01. TNF-α, tumor necrosis factor α; IL-6, interleukin-6; WT, wild-type; mKO, *miR-144/451* knockout; CLP, cecal ligation and puncture; ELISA, enzyme-linked immunosorbent assay.

Statistical analysis

Statistical analyses were performed using Microsoft Office Excel 2016 (Microsoft Corporation, Redmond, WA, USA). Data are presented as the mean ± standard deviation. Differences were assessed using two-tailed Student's *t*-tests. Differences were considered statistically significant when P<0.05.

Results

Decreased survival of sepsis-induced mKO mice

To determine the effects of *miR-144/451* on sepsis, we used mKO mice. After lethal sepsis was induced by CLP surgery (*Figure 1A*), the 48-hour survival rate in the WT group was 55.6%. However, the survival rate of mKO mice was 12.5%. These results suggested that the loss of *miR-144/451* may have contributed to severe sepsis-induced lethality.

Increased plasma TNF-α and IL-6 levels in mKO mice during sepsis

Levels of TNF-α and IL-6 in plasma which are critical markers of sepsis, were measured 12 hours post sepsis induction to assess the degree of systemic inflammatory response. Compared with the sham group, sepsis resulted in a significant increase in the levels of TNF-α and IL-6 in plasma (*Figure 1B,1C*). When comparing the sepsis groups to each other, plasma TNF-α and IL-6 levels were higher in mKO mice than WT mice.

Increased pulmonary permeability in mKO mice

Evans blue extravasation was used to assess the disruption of endothelial and epithelial barriers. Sham operation did not have a significant effect on Evans blue extravasation, whereas CLP surgery significantly induced extravasation. Evans blue exudation after CLP was enhanced in mKO mice compared to WT mice (*Figure 2A*).

Increased epithelial apoptosis in lung tissues of mKO mice

WT and mKO mice in the sham group displayed normal lung structures (*Figure 2B*). Lung tissues of mice in the sepsis groups exhibited interstitial haemorrhage and collapsed alveolar sacs. The capillaries in the alveolar walls were congested with neutrophils (*Figure 2B*). Sepsis-induced mKO lung tissues had more haemorrhage and were infiltrated with more neutrophils (*Figure 2B*), suggesting more severe injury than sepsis-induced WT mice.

Lung epithelial apoptosis was evaluated by TUNEL staining. Extensive apoptosis in the airway was detected in the CLP-induced mice. CLP-operated mKO mice showed an increased number of TUNEL-positive cells compared to control WT mice (*Figure 3A*).

Additionally, IHC was used to examine *Bax* protein expression in epithelial cells. CLP surgery significantly increased *Bax* protein levels in mKO mice compared to WT mice after CLP surgery (*Figure 3B*). Similarly, CLP surgery significantly elevated *Bax* mRNA levels and decreased *Bcl2* mRNA levels, whereas *miR-144/451* gene KO upregulated
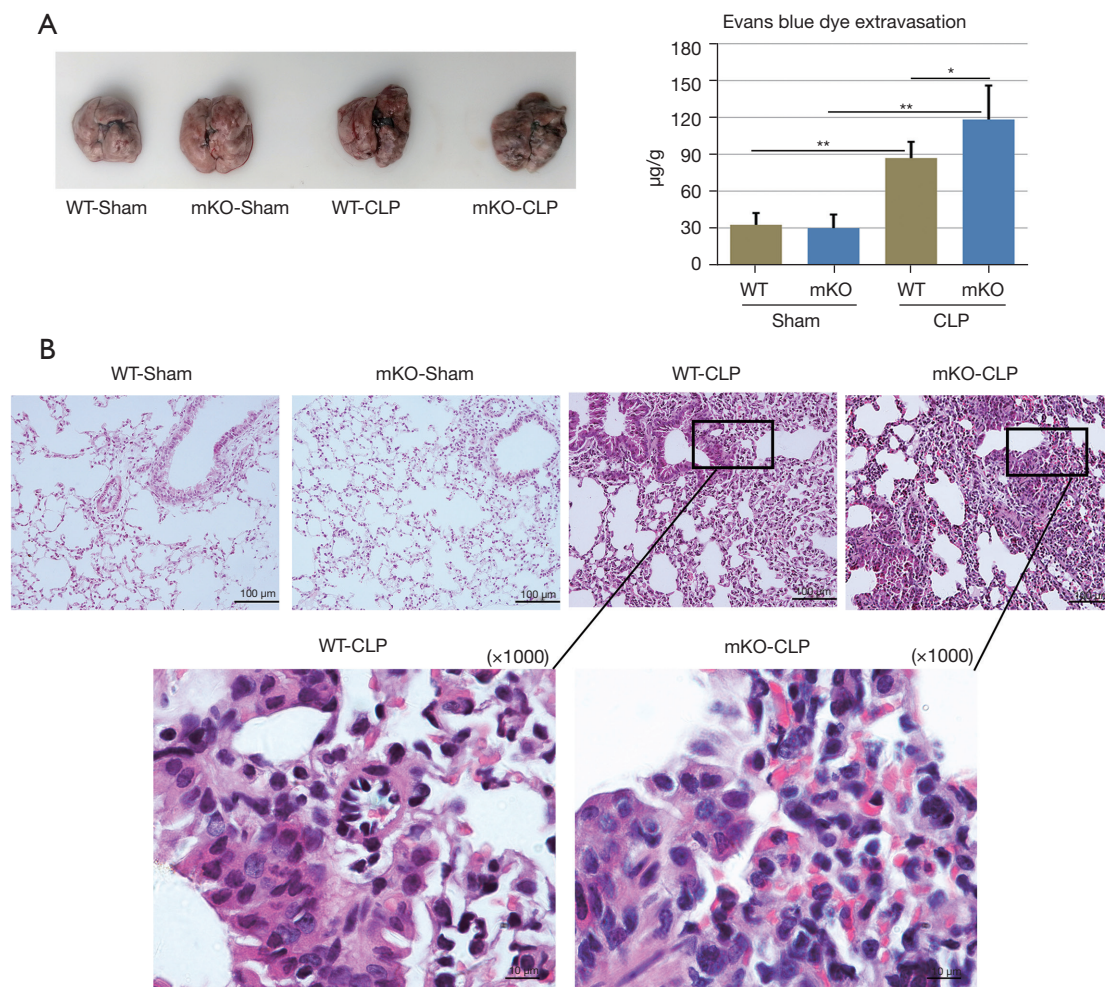
Figure 2 Sepsis-induced histopathological alterations in lung tissues and pulmonary permeability in WT and mKO mice. (A) Evans blue dye extravasation. (B) HE staining showing lung injury (200×, scale bar =100 µm). The magnified images (1,000×) represent the small squares outlined in the CLP groups. *P<0.05; **P<0.01. WT, wild-type; mKO, *miR-144/451* knockout; HE, hematoxylin-eosin; CLP, cecal ligation and puncture.

Bax mRNA and downregulated *Bcl2* transcription in septic mice (*Figure 4A,4B*).

Decreased antioxidant enzyme activity in the lungs of mKO mice

The activities of the Cat and Gpx1 enzymes in lung tissues were remarkably decreased after sepsis challenge in mKO mice compared to WT mice (*Figure 4C,4D*), indicating the insufficient antioxidant ability of mKO mice.

Downregulation of miR-451 expression in mouse lungs after severe sepsis

The levels of mature *miR-144* and *miR-451* in lung tissues with CLP-induced sepsis were measured. *MiR-451* was downregulated and *miR-144* was upregulated in lung tissues with CLP-induced sepsis compared to the sham group (*Figure 5A,5B*), suggesting that reduction of *miR-451* levels in the lung might have contributed to lethal sepsis-induced epithelial injury.
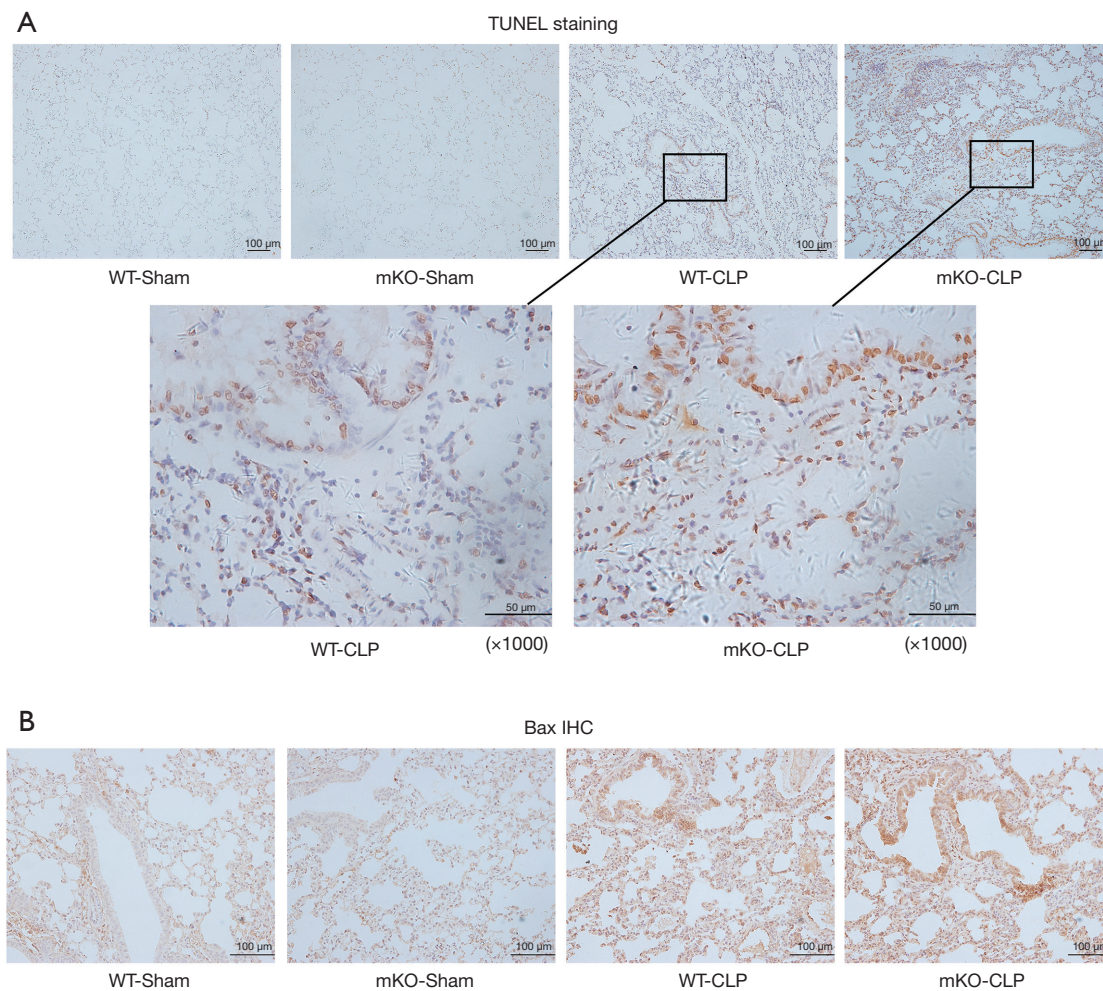
Figure 3 Sepsis-induced epithelial cell apoptosis in lung tissues in WT and mKO mice. (A) TUNEL staining showing cell apoptosis (100×, scale bar =200 µm). The magnified images (1,000×) represent the small squares outlined in the cecal ligation and puncture (CLP) groups. (B) IHC staining to examine Bax protein expression in lung tissues (200×, scale bar =100 µm). WT, wild-type; mKO, *miR-144/451* knockout; TUNEL, terminal deoxynucleotidyl transferase dUTP nick-end labeling; CLP, cecal ligation and puncture; IHC, immunohistochemistry; Bax, Bcl-2-associated X.

Overexpression of miR-451 suppressed LPS-induced cell apoptosis and increased antioxidant capacity in A549 cells

We performed additional *in vitro* experiments to illustrate the effect of *miR-451* overexpression on cell apoptosis and the antioxidant capacity in LPS-induced A549 cells. Upon LPS stimulation, A549 cells and those infected with retroviral supernatant containing the MSCV-PIG empty vector showed similar *miR-451* levels, whereas MSCV-*miR-451* infection significantly increased the expression of *miR-451* (*Figure 6A,6B*).

Cells that were positive for Annexin V-FITC and negative for PI were considered early apoptotic cells. LPS stimulated apoptosis in A549 cells and MSCV-*miR-451* infection decreased the percentage of early apoptotic cells (*Figure 6C,6D*). Further, *Bax* mRNA levels in A549 cells increased significantly after LPS stimulation, while *miR-451* overexpression significantly reduced *Bax* mRNA levels (*Figure 6E*). The levels of *Bcl2* mRNA also increased significantly in response to *miR-451* overexpression when LPS was administered (*Figure 6F*).

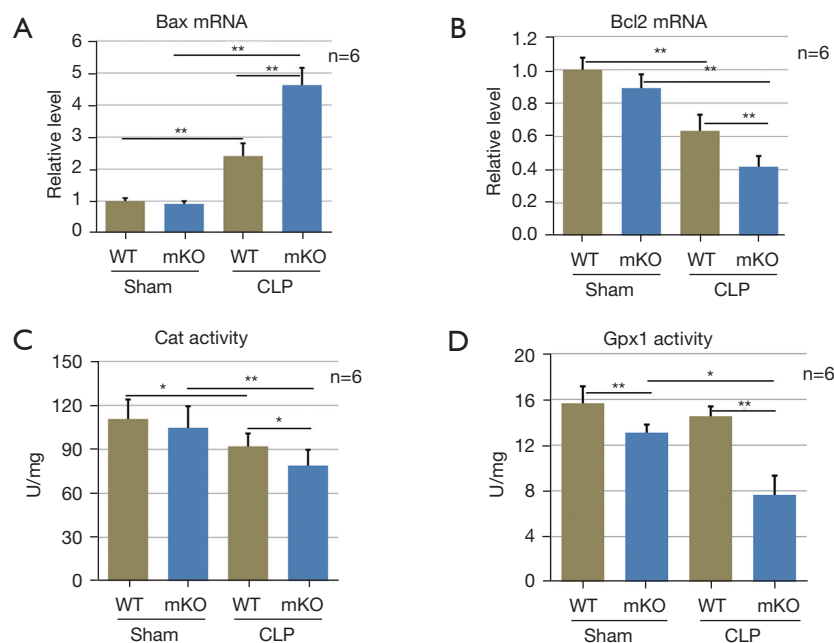Compared with the control group, ectopic expression of

Figure 4 Sepsis-induced changes in apoptosis-related gene expression and activity of antioxidant enzymes in lung tissues of WT and mKO mice. The levels of *Bax* (A) and *Bcl2* (B) mRNAs in lung tissues as determined by qRT-PCR. (C) Cat activity in lung tissues. (D) Gpx1 activity in lung tissues. Data are represented as means ± SD (n=6). *P<0.05; **P<0.01. WT, wild-type; mKO, *miR-144/451* knockout; *Bax*, Bcl-2-associated X; mRNAs, messenger RNAs; qRT-PCR, quantitative real-time polymerase chain reaction; Cat, catalase; Gpx1, glutathione peroxidase 1.
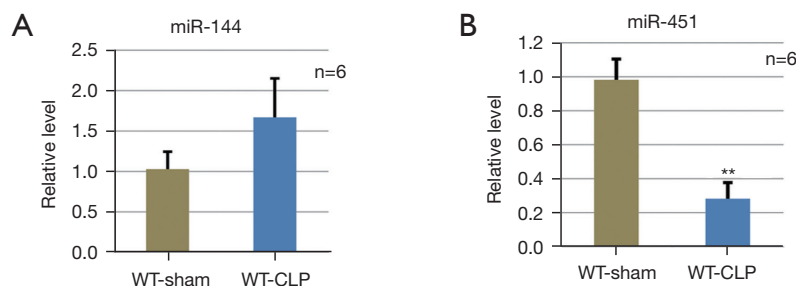
Figure 5 *miR-451* and *miR-144* expression in mouse lung tissues. The levels of *miR-144* (A) and *miR-451* (B) in the lung tissues of CLP-induced sepsis mice (n=6). Data are represented as means ± SD. **P<0.01. WT, wild-type; CLP, cecal ligation and puncture.

miR-451 enhanced the mRNA levels of antioxidant enzymes (Cat and Gpx1), indicating a positive role of *miR-451* in detoxifying ROS in A549 cells (*Figure 6G,6H*).

For ROS detection, A549 cells with or without *miR-451* mimics were incubated with DCFH-DA, and DCF fluorescence intensities were measured using flow cytometer. Compared with the control group, *miR-451* overexpression decreased intracellular ROS levels after LPS stimulation of A549 cells (Figure S1A,1B).

The miR-144/451-mediated 14-3-3ζ/FoxO3 pathway is involved in sepsis-induced epithelial oxidative stress

In our previous work, we demonstrated that 14-3-3ζ was a direct target of *miR-451* (18). 14-3-3ζ expression was upregulated in lung tissues of mKO mice (*Figure 7A*). Ectopic expression of *miR-451* in A549 cells significantly decreased *14-3-3ζ* protein levels (*Figure 7B*). These results suggested that miR-451 inhibited *14-3-3ζ* expression in
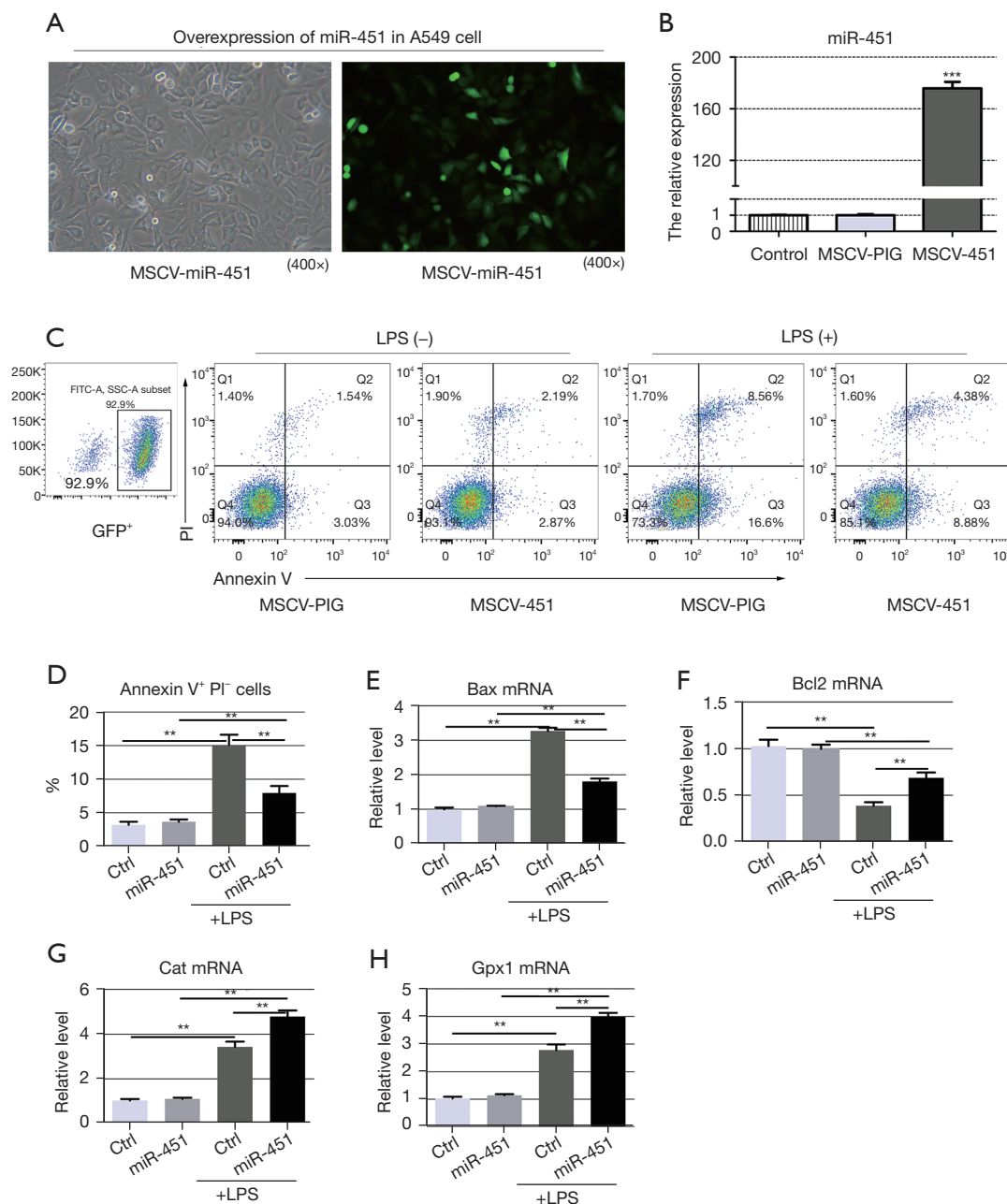
Figure 6 *miR-451* overexpression reduces cell apoptosis and mRNA levels of antioxidant enzymes in LPS-induced A549 cells. HEK293T cells were transfected with MSCV-PIG and MSCV-*miR-451* retroviral vectors and the A549 cells were infected with retroviruses. (A,B) *miR-451* levels after infection. MSCV-PIG (Puromycin IRES GFP) and MSCV-*miR-451* plasmids contain the sequence of green fluorescence protein, so cells infected with retroviral supernatant exhibit green fluorescence under a fluorescence microscope. (C,D) Flow cytometric analysis of apoptosis after LPS stimulation. The levels of *Bax* (E), *Bcl2* (F), *Cat* (G), and *Gpx1* (H) mRNAs in A549 cells as determined by qRT-PCR. Data are represented as means ± SD (n=3). **P<0.01; ***P<0.001. mRNA, messenger RNA; LPS, lipopolysaccharide; *Bax*, Bcl-2-associated X; *Cat*, catalase; *Gpx1*, glutathione peroxidase 1; qRT-PCR, quantitative real-time polymerase chain reaction.
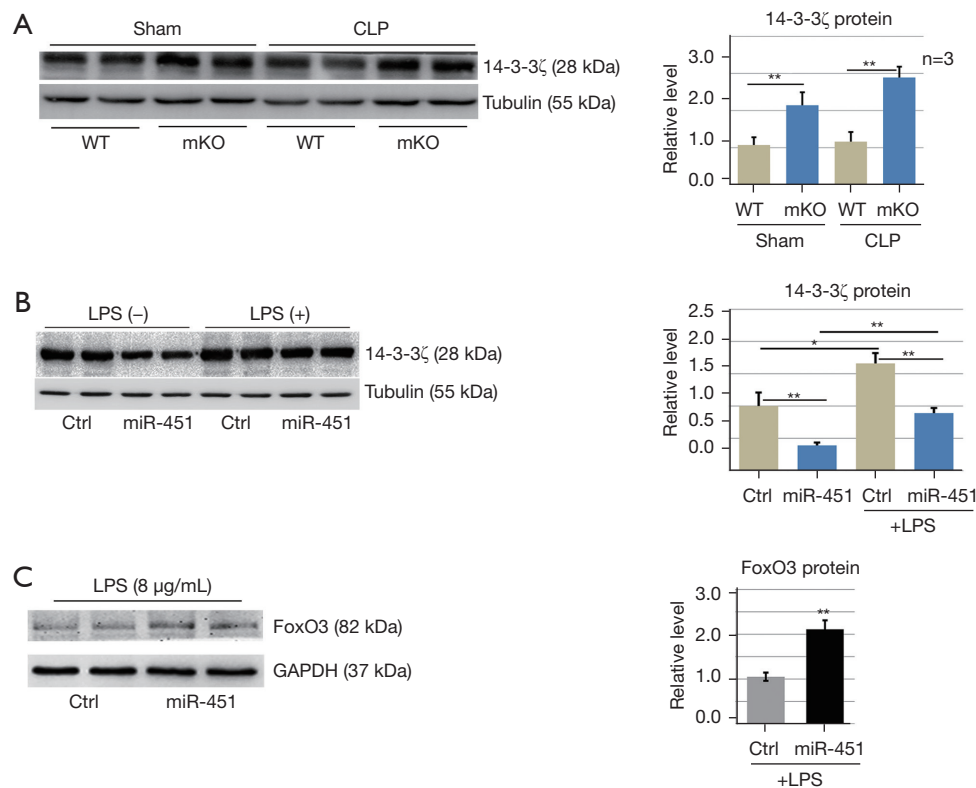
Figure 7 *MiR-451* negatively regulates the expression of 14-3-3ζ. (A) The *14-3-3ζ* protein levels in lung tissues of sepsis-induced WT and mKO mice as measured by western blot. The protein levels of *14-3-3ζ* (B) and nuclear *FoxO3* (C) in A549 cells treated with or without *miR-451* overexpression. Data are represented as means ± SD (n=3). *P<0.05; **P<0.01. WT, wild-type; mKO, *miR-144/451* knockout; CLP, cecal ligation and puncture groups; LPS, lipopolysaccharide.

lung epithelial cells. Further, we examined the expression of FoxO3 in human alveolar epithelial cells by western blot. Overexpression of *miR-451* increased *FoxO3* protein levels in the nucleus (*Figure 7C*).

Discussion

In this study, we found that *miR-144/451* deletion was associated with increased systemic inflammation, lung permeability, lung epithelial oxidative stress, and apoptosis in sepsis-induced mice. *MiR-451* overexpression enhanced ROS scavenging and antioxidant defenses by suppressing 14-3-3ζ/FoxO3 signalling, thereby reducing LPS-induced apoptosis.

Sepsis initiates a complex immune response that varies over time, starting with an initial proinflammatory phase and progressing to immunosuppression (13). Severe sepsis is quickly followed by organ failure and shock. Due to pulmonary susceptibility, acute respiratory distress

syndrome is one of the common lethal complications of sepsis (29). When the patient suffers from sepsis, pulmonary capillary endothelium is damaged and vascular permeability increases. The accumulation of oxidants stimulates a cascade of lipid peroxidation reactions that initiate epithelial apoptosis and autophagy (11). A large amount of protein-rich exudate destroys the barrier of pulmonary epithelial cells and accumulates in alveoli, which reduces effective ventilation and results in refractory hypoxemia, this is known as acute lung injury (30). Acute lung injury caused by sepsis is common in intensive care unit, which leads to high mortality. There are not many special clinical treatments for acute lung injury and current treatment methods are mainly symptomatic treatment and supportive interventions. Antibiotics, mechanical ventilation, and vasopressors are used to relive respiratory distress (4). Antioxidant supplementation such as vitamin C and melatonin is helpful for sepsis patients (14). The CLP-induced mouse model is widely used to study the mechanisms of sepsis (31). Wang

et al. reported that mice with severe sepsis showed 50% mortality 36 hours after CLP (26). Pulmonary oxidative stress and neutrophil activation are important factors in the development of respiratory failure after acute lung injury and sepsis. In this study, we find that sepsis initiates a complicated immune response that varies over time, starting with an initial proinflammatory phase and progressing to immunosuppression. Oxidative stress is a key mechanism underlying epithelial dysfunction in sepsis. A significant increase in the levels of TNF-α and IL-6 in plasma were observed 12 hours post sepsis induction compared with the sham group. The activities of the Cat and Gpx1 enzymes in lung tissues were decreased after sepsis challenge, indicating the insufficiency of antioxidant ability. The subsequent accumulation of ROS leads to the disruption of epithelial barriers and epithelial apoptosis in lung tissues. In the present study, CLP challenge resulted in 44% mortality within 2 days and the survival time was shortened in mKO mice. Meanwhile, cytokines associated with systemic inflammation such as TNF-α and IL-6 were elevated in mKO mice. These results suggested that the loss of *miR-144/451* promoted the development of sepsis.

Oxidative stress is a key mechanism underlying epithelial dysfunction in sepsis. In most mammalian cells, hydrogen peroxide is primarily broken down by Cat and Gpx1 (32). ROS can induce cell damage by oxidizing DNA, lipids, and proteins under conditions where protective antioxidant mechanisms are compromised (33). ROS increases permeability in the airway epithelium and long-term, continuous exposure to hydrogen peroxide leads to the disruption of tight junction proteins in the 16HBE human bronchial epithelial cell line (34). LPS also directly induces apoptosis in the A549 human alveolar epithelial cell line through ROS-mediated activation of the intrinsic mitochondrion-cytochrome c-caspase protease (35). In severe cases, irreversible pulmonary damage may lead to respiratory failure. The lungs are highly susceptible to infection during the later immunosuppression phase of sepsis (13). Suppression of innate immune responses in the lung occurs as early as 12 hours after low-grade CLP (36). In our study, high-grade CLP induced immunosuppression, which was characterized by lymphopenia in the blood (data not shown).

MiR-144/451 has been previously implicated in pathogenic or allergen-induced epithelial injury. Ectopic expression of *miR-144* results in increased replication of the influenza virus, the encephalomyocarditis virus, and the vesicular stomatitis virus in primary mouse lung epithelial cells (19). *MiR-144* upregulation is significantly correlated with total cell counts from bronchoalveolar lavages in models of ovalbumin-induced airway inflammation (20). *MiR-144* is upregulated and inversely correlated with forced expiratory volume in 1 second forced expiratory volume (FEV1)% in chronic obstructive pulmonary disease patients. *MiR-144* knockdown relieves cigarette smoke extract-induced inflammatory injury by upregulating PHLPP2 in 16HBE cells (21). The up-regulated expression of miR-144-3p accelerates lung epithelial cell apoptosis by regulating AQP1 axis in the lipopolysaccharide-induced mouse model (37). Sputum and serum miR-144 levels are higher in the patients with tuberculosis (TB), but decrease after anti-TB treatment (38). miR-144 might involve in regulation of anti-TB immunity through modification of cytokine production and cell proliferation of T cells (39). miR-144 is highly expressed in lung samples from patients with severe chronic obstructive pulmonary disease (COPD) when compared to control groups (40). These results suggest that upregulation of *miR-144* in the lungs promotes inflammatory diseases. A recent study reported that lung inflammation and cell apoptosis induced by LPS were alleviated by injection of a *miR-144* antagomir (41). However, in our study, deletion of the *miR-144/451* cluster aggravated sepsis-induced lung epithelial injury, indicating that *miR-451* might have played a crucial role in determining sepsis severity.

MiR-451 is considered a tumor suppressor (42). Emerging studie26s have indicated that *miR-451* also plays an important role in maintaining physiological homeostasis in lungs. Rosenberger *et al.* reported that inhibition of *miR-451* in primary dendritic cells increased the secretion of IL-6, TNF, chemokine ligand 5 (CCL5)/RANTES, and CCL3/MIP1α after influenza infection (22). *MiR-451* is downregulated in alveolar macrophages and contributes to allergic airway inflammation (23). It is suggested that miR-451 may relieve chronic inflammatory pain by inhibiting microglia activation-mediated inflammation via targeting TLR4 in allergic asthma (43). MiR-451 is downregulated in docetaxel-resistant lung adenocarcinoma cells, and overexpression of miR-451 reverse epithelial-mesenchymal transition to mesenchymal-epithelial transition (MET) both *in vitro* and *in vivo* (44). miR-451 inhibits the aggressiveness of lung squamous cell carcinoma by regulating KIF2A (45). Plasma miR-451 is also markedly decreased in pulmonary hypertension patients (46).

In the present study, we find that the levels of miR-451 in the lungs are reduced and overexpression of miR-

451 is effective against oxidative cell death. FoxO3 is a member of the FOXO transcription factor family that controls signalling that is important to cellular homeostasis including energy production, cell viability and proliferation (47). *MiR-451* protects erythrocytes against oxidative stress through the 14-3-3ζ/FoxO3 pathway, which positively regulates the activity of Cat and Gpx1 in erythroid cells (18). Consistently, overexpression of *miR-451* decreases the levels of *14-3-3ζ* protein, increases nuclear accumulation of FoxO3, and enhances ROS scavenging, and thus prevents LPS-induced apoptosis. In this study, we discovered that deletion of the miR-144/451 cluster aggravates sepsis-induced lung epithelial oxidative stress and apoptosis; and miR-451/14-3-3ζ/FoxO3 pathway is involved to protect lung epithelial cells against oxidative stress. We have previously reported that miR-451 represses the LKB1/AMPK/mTOR pathway to promote erythroblast survival (24). Loss of *miR-144/451* de-represses the mRNA expression of *Cab39*, the target gene of *miR-451*, *and thus activates* Cab39/AMPK/mTOR pathway in miR-144/451$^{-/-}$ erythroblasts to induce apoptosis. It might be another possible mechanism that increases epithelial apoptosis in lung tissues, though it has not been confirmed. Here we just focus on a miR-451-dependent, 14-3-3ζ-mediated mechanism. However, whether miR-144 also impacts oxidative stress and apoptosis is not clear. It will be interesting to investigate the effects of miR-144 and miR-451 individually by examining mice that harbor single miRNA mutations.

In conclusion, our study has shown that deletion of the *miR-144/451* cluster aggravated sepsis-induced lung epithelial oxidative stress and apoptosis in mice. *MiR-451* overexpression reduced intracellular ROS levels by suppressing 14-3-3ζ/FoxO3 signalling in LPS-induced cells.

Acknowledgments

Footnote

References

1. Xie J, Wang H, Kang Y, et al. The Epidemiology of Sepsis in Chinese ICUs: A National Cross-Sectional Survey. Crit Care Med 2020;48:e209-18.
2. Salomão R, Ferreira BL, Salomão MC, et al. Sepsis: evolving concepts and challenges. Braz J Med Biol Res 2019;52:e8595.
3. Ziesmann MT, Marshall JC. Multiple Organ Dysfunction: The Defining Syndrome of Sepsis. Surg Infect (Larchmt) 2018;19:184-90.
4. Perner A, Rhodes A, Venkatesh B, et al. Sepsis: frontiers in supportive care, organisation and research. Intensive Care Med 2017;43:496-508.
5. Gauer R, Forbes D, Boyer N. Sepsis: Diagnosis and

Management. Am Fam Physician 2020;101:409-18.

6. Zampieri FG, Mazza B. Mechanical Ventilation in Sepsis: A Reappraisal. Shock 2017;47:41-6.

7. Nanchal RS, Truwit JD. Recent advances in understanding and treating acute respiratory distress syndrome. F1000Res 2018;7:eF1000 Faculty Rev-1322.

8. Bissonnette EY, Lauzon-Joset JF, Debley JS, et al. Cross-Talk Between Alveolar Macrophages and Lung Epithelial Cells is Essential to Maintain Lung Homeostasis. Front Immunol 2020;11:583042.

9. Sarma JV, Ward PA. Oxidants and redox signaling in acute lung injury. Compr Physiol 2011;1:1365-81.

10. Zhang L, Meng Q, Yepuri N, et al. Surfactant Proteins-A and -D Attenuate LPS-Induced Apoptosis in Primary Intestinal Epithelial Cells (IECs). Shock 2018;49:90-8.

11. Nagar H, Piao S, Kim CS. Role of Mitochondrial Oxidative Stress in Sepsis. Acute Crit Care 2018;33:65-72.

12. Chawla LS, Fink M, Goldstein SL, et al. The epithelium as a target in sepsis. Shock 2016;45:249-58.

13. Venet F, Monneret G. Advances in the understanding and treatment of sepsis-induced immunosuppression. Nat Rev Nephrol 2018;14:121-37.

14. Prauchner CA. Oxidative stress in sepsis: Pathophysiological implications justifying antioxidant co-therapy. Burns 2017;43:471-85.

15. Finicelli M, Squillaro T, Galderisi U, et al. Micro-RNAs: Crossroads between the Exposure to Environmental Particulate Pollution and the Obstructive Pulmonary Disease. Int J Mol Sci 2020;21:7221.

16. Mohan A, Agarwal S, Clauss M, et al. Extracellular vesicles: novel communicators in lung diseases. Respir Res 2020;21:175.

17. Rajasekaran S, Pattarayan D, Rajaguru P, et al. MicroRNA Regulation of Acute Lung Injury and Acute Respiratory Distress Syndrome. J Cell Physiol 2016;231:2097-106.

18. Yu D, dos Santos CO, Zhao G, et al. miR-451 protects against erythroid oxidant stress by repressing 14-3-3zeta. Genes Dev 2010;24:1620-33.

19. Rosenberger CM, Podyminogin RL, Diercks AH, et al. miR-144 attenuates the host response to influenza virus by targeting the TRAF6-IRF7 signaling axis. PLoS Pathog 2017;13:e1006305.

20. Bartel S, Schulz N, Alessandrini F, et al. Pulmonary microRNA profiles identify involvement of Creb1 and Sec14l3 in bronchial epithelial changes in allergic asthma. Sci Rep 2017;7:46026.

21. Wang M, Liu Y, Zhang Y, et al. LncRNA LOC729178 acts as a sponge of miR-144-3p to mitigate cigarette smoke extract-induced inflammatory injury via regulating PHLPP2 in 16HBE cells. J Mol Histol 2021;52:437-47.

22. Rosenberger CM, Podyminogin RL, Navarro G, et al. miR-451 regulates dendritic cell cytokine responses to influenza infection. J Immunol 2012;189:5965-75.

23. Chung S, Lee YG, Karpurapu M, et al. Depletion of microRNA-451 in response to allergen exposure accentuates asthmatic inflammation by regulating Sirtuin2. Am J Physiol Lung Cell Mol Physiol 2020;318:L921-30.

24. Fang X, Shen F, Lechauve C, et al. miR-144/451 represses the LKB1/AMPK/mTOR pathway to promote red cell precursor survival during recovery from acute anemia. Haematologica 2018;103:406-16.

25. Xu L, Wu F, Yang L, et al. miR-144/451 inhibits c-Myc to promote erythroid differentiation. FASEB J 2020;34:13194-210.

26. Wang X, Huang W, Yang Y, et al. Loss of duplexmiR-223 (5p and 3p) aggravates myocardial depression and mortality in polymicrobial sepsis. Biochim Biophys Acta 2014;1842:701-11.

27. Wang W, Liu Z, Su J, et al. Macrophage micro-RNA-155 promotes lipopolysaccharide-induced acute lung injury in mice and rats. Am J Physiol Lung Cell Mol Physiol 2016;311:L494-506.

28. Fang L, Gao Y, Liu F, et al. Shuang-huang-lian attenuates lipopolysaccharide-induced acute lung injury in mice involving anti-inflammatory and antioxidative activities. Evid Based Complement Alternat Med 2015;2015:283939.

29. Li R, Ren T, Zeng J. Mitochondrial Coenzyme Q Protects Sepsis-Induced Acute Lung Injury by Activating PI3K/Akt/GSK-3β/mTOR Pathway in Rats. Biomed Res Int 2019;2019:5240898.

30. Mowery NT, Terzian WTH, Nelson AC. Acute lung injury. Curr Probl Surg 2020;57:100777.

31. Toscano MG, Ganea D, Gamero AM. Cecal ligation puncture procedure. J Vis Exp 2011;(51):2860.

32. Forkink M, Smeitink JA, Brock R, et al. Detection and manipulation of mitochondrial reactive oxygen species in mammalian cells. Biochim Biophys Acta 2010;1797:1034-44.

33. Hussain T, Tan B, Yin Y, et al. Oxidative Stress and Inflammation: What Polyphenols Can Do for Us? Oxid Med Cell Longev 2016;2016:7432797.

34. Chapman KE, Waters CM, Miller WM. Continuous exposure of airway epithelial cells to hydrogen peroxide: protection by KGF. J Cell Physiol 2002;192:71-80.

35. Chuang CY, Chen TL, Cherng YG, et al.

Lipopolysaccharide induces apoptotic insults to human alveolar epithelial A549 cells through reactive oxygen species-mediated activation of an intrinsic mitochondrion-dependent pathway. Arch Toxicol 2011;85:209-18.

36. Grailer JJ, Kalbitz M, Zetoune FS, et al. Persistent neutrophil dysfunction and suppression of acute lung injury in mice following cecal ligation and puncture sepsis. J Innate Immun 2014;6:695-705.

37. Li H, Shi H, Gao M, et al. Long non-coding RNA CASC2 improved acute lung injury by regulating miR-144-3p/AQP1 axis to reduce lung epithelial cell apoptosis. Cell Biosci 2018;8:15.

38. Lv Y, Guo S, Li XG, et al. Sputum and serum microRNA-144 levels in patients with tuberculosis before and after treatment. Int J Infect Dis 2016;43:68-73.

39. Liu Y, Wang X, Jiang J, et al. Modulation of T cell cytokine production by miR-144* with elevated expression in patients with pulmonary tuberculosis. Mol Immunol 2011;48:1084-90.

40. Hassan F, Nuovo GJ, Crawford M, et al. MiR-101 and miR-144 regulate the expression of the CFTR chloride channel in the lung. PLoS One 2012;7:e50837.

41. Xu R, Shao Z, Cao Q. MicroRNA-144-3p enhances LPS induced septic acute lung injury in mice through downregulating Caveolin-2. Immunol Lett 2021;231:18-25.

42. Bai H, Wu S. miR-451: A Novel Biomarker and Potential Therapeutic Target for Cancer. Onco Targets Ther 2019;12:11069-82.

43. Sun X, Zhang H. miR-451 elevation relieves inflammatory pain by suppressing microglial activation-evoked inflammatory response via targeting TLR4. Cell Tissue Res 2018;374:487-95.

44. Chen D, Huang J, Zhang K, et al. MicroRNA-451 induces epithelial-mesenchymal transition in docetaxel-resistant lung adenocarcinoma cells by targeting proto-oncogene c-Myc. Eur J Cancer 2014;50:3050-67.

45. Uchida A, Seki N, Mizuno K, et al. Regulation of KIF2A by Antitumor miR-451a Inhibits Cancer Cell Aggressiveness Features in Lung Squamous Cell Carcinoma. Cancers (Basel) 2019;11:258.

46. Song XW, Zou LL, Cui L, et al. Plasma miR-451 with echocardiography serves as a diagnostic reference for pulmonary hypertension. Acta Pharmacol Sin 2018;39:1208-16.

47. Link W. Introduction to FOXO Biology. Methods Mol Biol 2019;1890:1-9.

Table S1 Primer sequences for qRT-PCR

| Gene	Forward	Reverse
miR-451	AAACCGTTACCATTACTGAGT	Universal
miR-144	TACAGTATAGATGATGTACT	Universal
U6	CGCTTCGGCAGCACATATAC	Universal
mus-GAPDH	AATGGTGAAGGTCGGTGTGA	CTCCTGGAAGATGGTGATGG
mus-Bax	GGTTTCATCCAGGATCGAGCA	CGTCAGCAATCATCCTCTGCA
mus-Bcl2	GCTACCGTCGTGACTTCGC	CCCCACCGAACTCAAAGAAGG
has-Bax	AGCGACTGATGTCCCTGTCTCC	AGATGGTGAGTGAGGCGGTGAG
has-Bcl2	TCGCCCTGTGGATGACTGAGTAC	ACAGCCAGGAGAAATCAAACAGAGG
has-Cat	AATGAAAAACAGTCGTGTACCG	CCTTCTGCAACTGATCTACTGA
has-Gpx1	ACAAGCGCTTCTACTTAGATGT	GTAGTGTTCTATGAAGTCGCCC
hsa-GAPDH	GTCATGGGTGTGAACCATGA	ACTGTGGTCATGAGTCCTTC

qRT-PCR, quantitative real-time PCR.
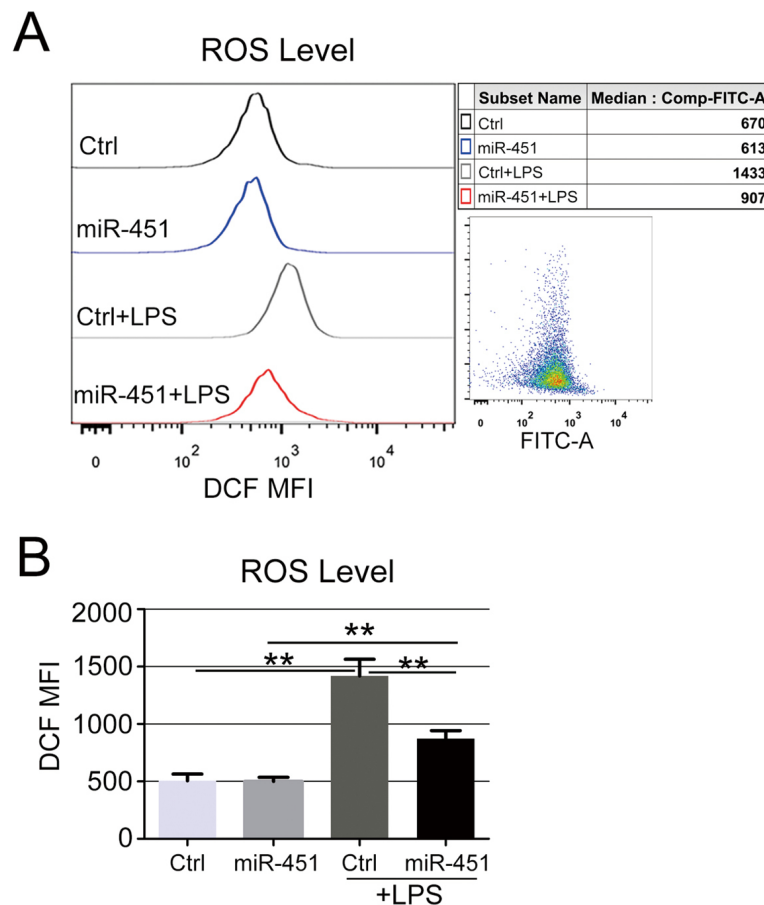
Figure S1 *MiR-451* overexpression decreases intracellular reactive oxygen species (ROS) levels after lipopolysaccharide (LPS) stimulation. A549 cells were transfected with *miR-451* mimic and miR-NC. (A) ROS levels were determined by flow cytometry and measured by the mean fluorescence intensity (MFI) of dichloro-dihydro-fluorescein (DCF). (B) Quantitative analysis of MFI for DCF. **P<0.01.